

Semi-classical calculations of self-broadening coefficients of OCS and HCN at temperatures between 200 K and 298 K



C. Jellali ^{a,*}, S. Galalou ^a, A. Cuisset ^{b,c}, M. Dhib ^a, H. Aroui ^a

^a Laboratoire de Dynamique Moléculaire et Matériaux Photoniques, Université de Tunis, Ecole Nationale Supérieure d'Ingénieurs de Tunis, 5 Av. Taha Hussein, Tunis, Tunisia

^b Laboratoire de Physico-Chimie de l'Atmosphère EA 4493, Univ. Littoral Côte d'Opale, 59140 Dunkerque, France

^c Université de Lille, F-59000 Lille, France

ARTICLE INFO

Article history:

Received 30 June 2016

In revised form 19 August 2016

Accepted 22 August 2016

Available online 24 August 2016

Keywords:

Self-broadening coefficients

Hydrogen cyanide

Carbonyl sulfide

Semiclassical calculations

Exact trajectory

ABSTRACT

For some temperatures of atmospheric interest from 200 to 298 K, the self-broadening coefficients of OCS-OCS and HCN-HCN collisional systems, at different strengths of electrostatic interactions, were calculated respectively for ν_1 and ν_2 bands for a wide range of rotational quantum numbers J . In particular, we have considered some lines that were not studied previously. We have employed the approximation of bi-resonance functions (Starikov, 2012) in the frame of the semiclassical model of Robert and Bonamy with exact trajectory (RBE).

The calculated results are found to be fully consistent with the available experimental values of self-broadening coefficients of OCS and HCN. A comparative study shows that the RBE calculations reproduce the dependence of broadening coefficients on quantum number J much better than the simpler Robert and Bonamy model with parabolic trajectory (RB) for all considered temperatures.

© 2016 The Authors. Published by Elsevier Inc. This is an open access article under the CC BY-NC-ND license (<http://creativecommons.org/licenses/by-nc-nd/4.0/>).

1. Introduction

At room temperature, the semiclassical formalism of Robert and Bonamy with parabolic trajectory RB [2] has produced reliable results of collisional broadening coefficients of OCS perturbed by O_2 and N_2 [3,4]. But, this model led to a relatively poor agreement with experimental data for OCS-OCS [5,6] collisional system for the two temperatures 200 and 298 K. Ross and Willey [7] compared theoretical results derived from quantum calculations to the measured broadening coefficients of OCS perturbed by He from 4.2 to 23 K for the rotational lines R(1), R(2) and R(3). The measurements were realized in quasi-equilibrium cell employing the collisional cooling technique. The calculations of pressure broadening coefficients were performed using an ab initio He-OCS potential surface. A significant disagreement between theoretical and experimental coefficients increasing with decreasing temperature was clearly observed.

Using the RB formalism, Bouanich et al. [8] have calculated the self-broadening coefficients in the ν_2 band of HCN for temperature ranging from 212 to 296 K. The intermolecular potential used in

this calculation was purely electrostatic. The theoretical results were found to be consistent with the experimental data of Malathy Devi et al. [9].

The exact trajectory model leads to a significantly improved version of the RB formalism [10]. It involves the exact solutions of the classical equations of motion [11]. It led to good results for HCN perturbed by N_2 at room temperature [12]. Yang et al. [12] were the first who computed the rotational lines of HCN perturbed by O_2 . This computation introduced the original integral formula of resonance functions. This model can be a suitable alternative to calculate pressure broadening coefficients and to study their temperature dependences. Indeed, this version of the RB formalism was applied with success to many collisional systems such as CH_3D-CH_3D [13], CH_3D-N_2 [13] and CH_3Cl -air [14] at various temperatures.

Using the Anderson-Tsao-Curnutte [15] and RB models, Bouanich et al. have calculated [5,6] self broadening coefficients for 70 lines in the ν_1 band of OCS at 200 and 298 K.

Rinsland et al. [16] have measured the air- and N_2 broadening coefficients, and the temperature exponent dependence for the lines of the ν_1 band of HCN. These parameters were determined for J up to 29 at temperatures between 213 and 299 K. Smith et al. [17] have measured the N_2 broadening coefficients of HCN and their temperature exponent dependence for ν_2 band

* Corresponding author.

E-mail address: chakerjellali@yahoo.fr (C. Jellali).

at temperatures between 211 and 300 K. Using two different Fourier transform spectrometers (FTS), the McMath-Pierce FTS and the Bruker IFS 120HR FTS, Malathy Devi et al. [9,18] have determined the self- and air broadening coefficients of HCN at various temperatures of atmospheric interest between 212 and 296 K for lines belonging to the P- and R-branches of the ν_1 and ν_2 bands. Yang et al. [12] have measured the rotational lines widths of HCN perturbed by O_2 , N_2 and air at room-temperature by continuous-wave terahertz (CW-THz) spectrometry. Self-broadening coefficients for pure rotational lines of OCS have been measured at room temperature for high J values up to 90 by Matton et al. [19] and refined values were determined by Koshelev et al. [20]. In this last study, theoretical calculations of self-broadening parameters were performed in the framework of the RB formalism where the speed dependence on the line profiles were considered.

In the present work, we have computed HCN and OCS self-broadening coefficients using the RBE formalism. The predicted values are compared to experimental results for 54 lines of the ν_2 band of HCN [9] at temperatures between 212 and 296 K, and for 46 lines belonging to the ν_1 band [6] of OCS at 200 and 298 K.

2. Theory and computational method

2.1. Theory

Recently, Bykov et al. [10] have proposed exact solutions of the equations of motion for a particle in an isotropic potential field. They have defined a special integral form for resonance functions used in the calculation of pressure broadening coefficients. For the case of two linear molecules, this approach has been already discussed in details in Ref. [21].

To employ the model of exact trajectory, the interaction potential must be put in the form invariant under overall rotations of the system:

$$V_{\text{aniso}}(\vec{r}) = \sum_{\ell_1 \ell_2 \ell} v_{\ell_1 \ell_2 \ell}(r) \sum_{m_1 m_2 m} C_{\ell_1 m_1 \ell_2 m_2}^m Y_{\ell_1}^{m_1}(\theta_1, \varphi_1) Y_{\ell_2}^{m_2}(\theta_2, \varphi_2) \bar{C}_{\ell m}^*(\theta, \Psi). \quad (1)$$

This expansion into a series of three spherical harmonics tied to the orientations of both molecular axes ($Y_{\ell_1}^{m_1}(\theta_1, \varphi_1)$, $Y_{\ell_2}^{m_2}(\theta_2, \varphi_2)$) and the intermolecular distance vector \vec{r} ($\bar{C}_{\ell m}(\theta, \Psi) = [4\pi/\sqrt{2\ell+1}]^{1/2} Y_{\ell}^m(\theta, \Psi)$) in the laboratory-fixed frame enables the separation of the angular (spherical harmonics) and radial ($v_{\ell_1 \ell_2 \ell}(r)$) dependences of the interaction potential energy. $\ell = \ell_1 + \ell_2$, where the values of ℓ_1 and ℓ_2 depend on the type of molecular interactions (electrostatic, dispersion...).

In the frame of semi-classical Robert and Bonamy formalism [2], the pressure broadening coefficients γ of an optical transition $i \rightarrow f$ is given by:

$$\gamma = \frac{n}{2\pi c} \sum_{j_2} \rho_{j_2} \times \int_0^{+\infty} v F(v) dv \int_{r_{c0}}^{+\infty} 2\pi r_c \left(1 - V^*(r_c) - \frac{r_c}{2} V'^*(r_c)\right)^2 S_R(r_c, v) dr_c, \quad (2)$$

where n is the number density of perturbing gas, v is the relative velocity between the absorber and the perturber, $F(v)$ is the Maxwell velocity distribution, ρ_{j_2} is the relative population of the label of rotational level j_2 of the ground state of the perturber, and is the value of the position for the distance of closest approach.

$V^*(r_c) = V_{\text{iso}}(r_c)/mv^2$ is the normalized isotropic potential and the prime denotes derivation. For the exact trajectory governed by the intermolecular isotropic potential $V_{\text{iso}}(r_c)$, r_{c0} can be derived numerically from the following equation [22]:

$$\frac{2V_{\text{iso}}(r_{c0})}{mv^2} - 1 = 0 \quad (3)$$

The real part of differential broadening cross sections is given by [2]:

$$S_R(r_c, v) = 1 - \exp(\text{Re}S_2(r_c, v)), \quad (4)$$

where $S_2(r_c, v)$ results from the integration of the intermolecular potential over time. It can be expressed by [23]:

$$S_2 = 2h^{-2} \left(\frac{r_c}{v}\right)^2 \sum_{\ell_1 \ell_2 \ell} \left[\sum_{j_i j_f} \left(C_{j_i 0 \ell_1 0}^{j_i 0}\right)^2 \left(C_{j_2 0 \ell_2 0}^{j_2 0}\right)^2 \ell_1 \ell_2 \ell f + \sum_{j_i j_f} \left(C_{j_i 0 \ell_1 0}^{j_i 0}\right)^2 \left(C_{j_2 0 \ell_2 0}^{j_2 0}\right)^2 \ell_1 \ell_2 \ell f - \sum_{j_2} (-1)^{j_2 + j_2'} \left(C_{j_2 0 \ell_2 0}^{j_2 0}\right)^2 D_{j_i j_f}^{(\ell_1) \ell_1 \ell_2 \ell f} \right]. \quad (5)$$

h is the Plank's constant, j_i and j_f are respectively the initial and final labels of the rotational levels of transition. The term $D_{j_i j_f}^{(\ell_1)}$ has the following expression:

$$D_{j_i j_f}^{(\ell_1)} = 2(-1)^{j_i + j_f} [(2j_i + 1)(2j_f + 1)]^{1/2} C_{j_i 0 \ell_1 0}^{j_i 0} C_{j_f 0 \ell_1 0}^{j_f 0} W(j_i j_f j_i j_f; 1 \ell_1), \quad (6)$$

where the terms $C_{j_m 0 \ell_n 0}^{j_m 0}$ are the Clebsch-Gordan coefficients, and $W(j_i j_f j_i j_f; 1 \ell_1)$ is a Racah coefficient [24].

The term $\ell_1 \ell_2 \ell f$ in Eq. (5) is the resonance function depending on v , r_c and resonance k_c given by:

$$k_c = \frac{r_c \omega_{j_i j_f j_i j_f}}{v}, \quad (7)$$

where $\omega_{j_i j_f j_i j_f}$ is the frequency of collisionally induced transition $i \rightarrow f$.

The real part of resonance function, introduced in the calculation of broadening coefficients, can be expressed as [23]:

$$\ell_1 \ell_2 \ell f = N \sum_{m=-\ell}^{\ell} I_{\ell m}^p I_{\ell m}^{p'}, \quad (8)$$

where N is a normalization term ($\ell_1 \ell_2 \ell f(k_c = 0) = 1$) and $*$ denotes complex conjugation. The integer numbers p and p' are the powers of the intermolecular distance $r(t)$. The $I_{\ell m}^p$ terms are given by [23]:

$$I_{\ell m}^p = \int_{-\infty}^{+\infty} dt \frac{\bar{C}_{\ell m}(\theta, \Psi(t))}{r(t)^p} e^{i\omega_{if} t}. \quad (9)$$

2.2. Computational method

Due to the High CPU cost, we have used a realistic approximation, without a noticeable loss of precision, which consists on the use of the bi-resonance functions model of Starikov [1] who has proposed some simple analytic formula of the functions $\ell_1 \ell_2 \ell f$ for some types of intermolecular interactions.

For the electrostatic interactions (dipole - dipole, dipole - quadrupole, quadrupole - dipole and quadrupole - quadrupole interactions), the resonance functions are given by:

$$f^{\text{elec}} = \frac{a_1}{\cosh^2(a_2(k_c - a_3))} + \frac{a_4}{\cosh^2(a_5(k_c - a_6))} \quad (10)$$

Table 1

Data used in the calculations of pressure broadening coefficients.

	OCS	HCN
B_0 (cm ⁻¹)	0.202856 [25]	1.478221 [31]
B (cm ⁻¹)	0.202251 [25]	1.478201 [32]
D_0 (10 ⁻⁸ cm ⁻¹)	4.341 [25]	2.927 [32]
μ (D)	0.694 [26]	2.915 [28]
Q (DÅ ³)	-0.786 [27]	3.1 [29]
ε (K)	335 [30]	149.7 [33]
σ (Å ³)	4.13 [30]	3.796 [33]
γ	0.299 [29] ^a	-

^a Calculated from polarizability values given in Ref. [29].

The resonance function $f^{\text{disp}}(k_c)$ associated to the dispersion term $\left(\frac{\sigma}{r_c}\right)^{12} P_2(\cos \theta)$ is given by:

$$f^{\text{disp}}(k_c) = \frac{a_1}{\cosh^2(a_2(k_c - a_3))}. \quad (11)$$

The parameters a_n are expressed by:

$$a_n = \frac{[a_{n1} + a_{n2}\lambda(\beta^{12} - \beta^6)]}{[1 + a_{n3}\lambda(5\beta^{12} - 2\beta^6)]}, \quad (12)$$

where $\beta = \frac{\sigma}{r_c}$ and $\lambda = \frac{8\varepsilon}{mV^2}$, ε and σ are the parameters of Lennard-Jones, and λ characterizes the temperature dependence of resonance functions.

The parameters a_{nk} were obtained by a least squares method by fitting the exact values of resonance functions defined by Eq. (8) by the two resonance functions models given by Eqs. (10) and (11). All these parameters are given in Ref. [1].

Due to the strong electrostatic interactions of HCN ($\mu = 2.915$ D and $Q = 3.1$ DÅ³), the anisotropic part of intermolecular potential used in the calculations of self-broadening coefficients of HCN is limited to the sum of electrostatic contributions given by:

$$V_{\text{elec}} = V_{\mu_1\mu_2} + V_{\mu_1Q_2} + V_{Q_1\mu_2} + V_{Q_1Q_2}. \quad (13)$$

For OCS-OCS system, we have used an intermolecular potential which anisotropic part contains the long-range electrostatic interactions and the dispersion term $\gamma_{\text{OCS}}(\sigma/r_c)^{12}P_2(\cos \theta)$. The electrostatic potential V_{elec} is the same as the one of Eq. (13). The anisotropic part is given by the following expression:

$$V_{\text{aniso}} = V_{\text{elec}} + \gamma_{\text{OCS}}(\sigma/r_c)^{12}P_2(\cos \theta). \quad (14)$$

The parameters used in the calculations are listed in Table 1. These calculations have been performed for the ν_1 band of OCS and for the ν_2 band of HCN. Therefore, we have considered the rotational spectroscopic constants B and D for these two bands. The dimensionless polarizability anisotropy γ of Table 1 is given by

$$\gamma = \frac{\alpha_{\perp} - \alpha_{\parallel}}{\alpha} \quad \text{where } \alpha = \frac{2\alpha_{\perp} + \alpha_{\parallel}}{3} \quad (\text{mean polarizability}). \quad (15)$$

For both interacting systems, the exact trajectories are governed by a 12-6 Lennard-Jones potential.

3. Results

The collisional broadening coefficients of OCS and HCN self-perturbed have been calculated using the semiclassical Robert and Bonamy formalism with exact trajectory. In

addition to the previous experimental results [6,9], these calculations were compared with theoretical results of Bouanich et al. [6,8].

3.1. HCN-HCN collisional system

Self-broadening coefficients of ν_2 band of HCN have been computed using RBE calculations at four temperatures ranging from 212 to 296 K.

To determine the experimental values of self-broadening coefficients at temperature T , we used the following power law:

$$\gamma_{\text{HCN}}(T) = \gamma_{\text{HCN}}(296) \left(\frac{296}{T}\right)^n, \quad (16)$$

where n is the temperature dependence exponent of self-broadening. Its values are determined by linear regression analysis of $\ln(\gamma_{\text{HCN}}(T)/\gamma_{\text{HCN}}(296))$ versus $\ln(296/T)$. The experimental values of this exponent are given by Ref. [9]. We define $T_0 = 296$ K as the reference temperature.

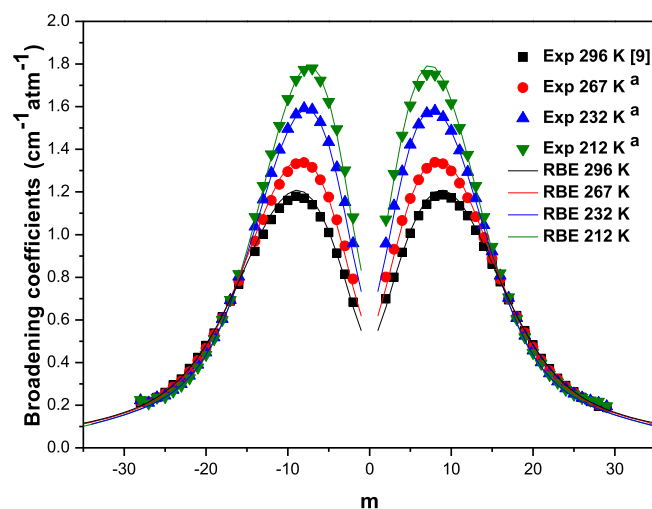


Fig. 1. Comparison between measured [9] and theoretical (present work) self-broadening coefficients of the ν_2 band of HCN. The experimental values at temperatures 267 K, 232 K and 212 K were deduced using Eq. (16) and measured values of n exponent of Ref. [9].

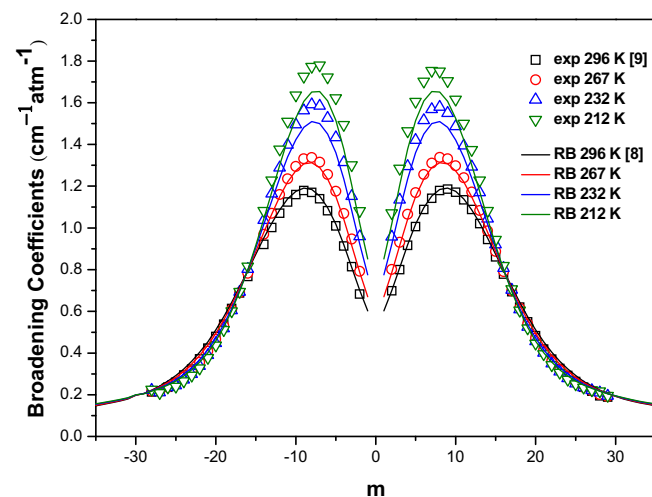


Fig. 2. Comparison between measured [9] and theoretical [8] self-broadening coefficients of the ν_2 band of HCN. The experimental and calculated values at temperatures 267 K, 232 K and 212 K were deduced using Eq. (16) and values of n exponent of Refs. [8,9].

Table 2
Theoretical and experimental values of self-broadening coefficients γ (T = 296 K) and temperature exponents n in the ν_2 band of HCN.

Lines	Broadening coefficients γ ($\text{cm}^{-1} \text{atm}^{-1}$)			Exponent n		
	γ_{Exp} [9]	γ_{RB} [8]	γ_{RBE}	n_{Exp} [9]	n_{RB} [8]	n_{RBE}
P(35)	–	0.1469	0.1153	–	–	–0.474
P(34)	–	0.1538	0.1237	–	–	–0.401
P(33)	–	0.1612	0.1328	–	–	–0.337
P(32)	–	0.1700	0.1427	–	–	–0.276
P(31)	–	0.1802	0.1536	–	–	–0.237
P(30)	–	0.1971	0.1659	–	–	–0.210
P(29)	–	0.2059	0.1799	–	–	–0.203
P(28)	0.2133	0.2222	0.1959	–0.070	0.160	–0.201
P(27)	0.2170	0.2415	0.2149	–0.144	–0.120	–0.223
P(26)	0.2356	0.2645	0.2371	–0.221	0.001	–0.261
P(25)	0.2598	0.2916	0.2635	–0.285	–0.245	–0.308
P(24)	0.2940	0.3238	0.2947	–0.331	–0.312	–0.223
P(23)	0.3220	0.3608	0.3317	–0.360	–0.294	–0.386
P(22)	0.3714	0.4043	0.3749	–0.378	–0.380	–0.416
P(21)	0.4237	0.4542	0.4253	–0.365	–0.341	–0.414
P(20)	0.4798	0.5109	0.4830	–0.330	–0.280	–0.414
P(19)	0.5384	0.5741	0.5482	–0.276	–0.154	–0.337
P(18)	0.6132	0.6435	0.6204	–0.197	–0.061	–0.252
P(17)	0.6882	0.7175	0.6986	–0.097	0.024	–0.136
P(16)	0.7673	0.7952	0.7811	0.016	0.180	0.001
P(15)	–	0.8736	0.8656	0.143	–	0.149
P(14)	0.9205	0.9507	0.9489	0.276	0.482	0.302
P(13)	1.0021	1.0232	1.0276	0.409	0.604	0.459
P(12)	1.0699	1.0873	1.0971	0.540	0.749	0.616
P(11)	1.1242	1.1394	1.1533	0.667	0.876	0.769
P(10)	1.1599	1.1753	1.1916	0.787	1.020	0.918
P(9)	1.1787	1.1916	1.2081	0.896	1.132	1.062
P(8)	1.1706	1.1851	1.1996	0.995	1.233	1.192
P(7)	1.1399	1.1538	1.1643	1.079	1.323	1.304
P(6)	1.0823	1.0975	1.1024	1.146	1.380	1.393
P(5)	1.0097	1.0181	1.0163	1.192	1.408	1.448
P(4)	0.9128	0.9201	0.9099	1.209	1.463	1.467
P(3)	0.8141	0.8103	0.7880	1.192	1.392	1.449
P(2)	0.6830	0.6994	0.6597	1.132	1.363	1.389
P(1)	–	0.6021	0.5489	1.037	–	1.279
R(0)	–	0.6021	0.5489	1.037	–	1.283
R(1)	0.6987	0.6994	0.6597	1.132	1.267	1.389
R(2)	0.7997	0.8102	0.7881	1.192	1.406	1.449
R(3)	0.9169	0.9200	0.9099	1.209	1.389	1.467
R(4)	1.0062	1.0180	1.0163	1.192	1.388	1.448
R(5)	1.0885	1.0974	1.1024	1.146	1.328	1.393
R(6)	1.1425	1.1537	1.1642	1.079	1.273	1.304
R(7)	1.1793	1.1850	1.1995	0.995	1.173	1.192
R(8)	1.1859	1.1914	1.2081	0.896	1.077	1.062
R(9)	1.1713	1.1752	1.1916	0.780	0.956	0.918
R(10)	1.1338	1.1392	1.1533	0.667	0.832	0.769
R(11)	1.0877	1.0871	1.0971	0.540	0.694	0.616
R(12)	1.0208	1.0230	1.0275	0.409	0.549	0.459
R(13)	0.9439	0.9505	0.9489	0.275	0.407	0.302
R(14)	0.8618	0.8734	0.8656	0.143	0.267	0.149
R(15)	0.7778	0.7950	0.7811	0.016	0.151	0.001
R(16)	0.6945	0.7173	0.6986	–0.097	0.049	–0.136
R(17)	0.6200	0.6433	0.6204	–0.198	–0.077	–0.252
R(18)	0.5486	0.5739	0.5482	–0.276	–0.168	–0.337
R(19)	0.4834	0.5108	0.4830	–0.331	–0.237	–0.387
R(20)	0.4185	0.4540	0.4253	–0.363	–0.170	–0.414
R(21)	0.3708	0.4041	0.3749	–0.378	–0.238	–0.416
R(22)	0.3260	0.3606	0.3317	–0.360	–0.187	–0.386
R(23)	0.2925	0.3236	0.2947	–0.331	–0.200	–0.342
R(24)	0.2624	0.2915	0.2635	–0.285	–0.135	–0.308
R(25)	0.2358	0.2644	0.2371	–0.221	–0.017	–0.261
R(26)	0.2170	0.2414	0.2149	–0.145	0.069	–0.223
R(27)	0.1939	0.2221	0.1960	–0.075	0.328	–0.202
R(28)	0.1885	0.2058	0.1799	–	0.113	–0.203
R(29)	–	0.1920	0.1658	–	–	–0.210
R(30)	–	0.1801	0.1536	–	–	–0.237
R(31)	–	0.1699	0.1427	–	–	–0.276
R(32)	–	0.1611	0.1328	–	–	–0.337
R(33)	–	0.1536	0.1237	–	–	–0.401
R(34)	–	0.1470	0.1153	–	–	–0.123

Figs. 1 and 2 present the comparison of theoretical results of self-broadening coefficients of HCN derived respectively from the RBE (present work) and RB calculations [8] with experimental data of Malathy Devi et al. [9]. The corresponding numerical results are given in Table 2.

Fig. 1 shows that RBE calculations reproduce nicely the rotational evolution of self-broadening coefficients of ν_2 band of HCN. These calculations lead to the best agreement with experimental data for the four temperatures 296 K, 267 K, 232 K and 212 K. In descending order of these temperatures, the difference on percent is about 1.6%, 1.9%, 3.5% and 2.9% for RBE calculations and about 4.6%, 4.2%, 4.7% and 5.0% for RB calculations [8].

In Fig. 1, for temperatures ranging from 212 to 296 K, the theoretical self-broadening coefficients, generated by RBE calculations for both R ($m = J + 1$) and P ($m = -J$) branches of ν_2 band, tend to increase until they reach a maximum, and then start to decrease in ascending order of J . The values of J_{\max} (equal to 7 at $T = 296$ K) which correspond to the maximum of contribution of the whole electrostatic interactions were consistent with experimental values for $T = 296$ K ($J_{\max} = 8$ for R branch and $J_{\max} = 9$ for P branch) as well as ones obtained using the resonance condition [5,34] of Eq. (17).

$$J_{\max} \approx \frac{B_1}{B_2} \frac{\ell_1}{\ell_2} J_{2p}, \quad (17)$$

where J_{2p} is the most populated level of the perturbing molecule at the considered temperature ($J_{2p} = 8$ for HCN for $T = 296$ K). B_1 and B_2 are the rotational constants of the two collisional partners ($B_1 = B_2$ for HCN self-perturbed). Therefore for the self broadening dominated by the dipole-dipole interaction ($\ell_1 = \ell_2 = 1$) as mentioned in Ref. [8], the maximum of collision effectiveness is around $J_{\max} = 8$.

Fig. 3 presents the variation of theoretical and experimental values of temperature dependence exponent n as function of the J rotational quantum number.

This figure shows that RBE and RB calculations reproduce nicely the evolution of exponent n as function of m and agree differently with experimental data. The theoretical values of n derived from

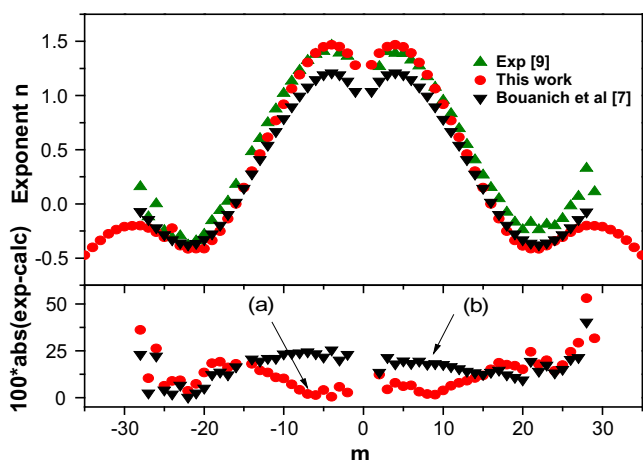


Fig. 3. Rotational dependence of temperature exponent in the ν_2 band of HCN. (a) Present work, (b) Bouanich et al. [8].

RBE formalism are closer to the experimental results for majority of lines especially for $|m| < 15$.

As illustrated by this figure, the exponent n of the R and P branches, decreases monotonically for $5 < J < 20$ until attaining an inflection point at about $J_{\text{inf}} = 16$ and becomes negative wherever $J > J_{\text{inf}}$. This behavior is not surprising since as seen in Fig. 1, the values of $\gamma_{\text{HCN}}(T)$ ($T = 212, 232$ and 267 K) become smaller than $\gamma_{\text{HCN}}(296)$ for $|m| > 16$.

Table 2 presents the values of self-broadening coefficients ($T = 296$ K) and temperatures exponents n obtained in this work as well as those reported in Refs. [8,9] corresponding to the ν_2 band of HCN.

3.2. OCS-OCS collisional system

We have computed the self-broadening coefficients of OCS for the temperatures 200 and 298 K.

The comparisons between the computed coefficients, derived from the RBE (present work) and RB calculations [6], and the experimental results [6] are shown in Fig. 4.

For these temperatures, the RBE calculations for both R and P branches of ν_1 reproduce the maximum of collision effectiveness which is around $J_{\max} = 24$ at temperature $T = 298$ K. This values is close to the experimental value of Ref. [6] which is around $J_{\max} = 24$ and to the one deduced from resonance condition given by Eq. (17) leading to $J_{\max} = 22$ and justifying that the self broadening of OCS is dominated by the dipole-dipole interaction ($\ell_1 = \ell_2 = 1$).

Also, we notice that within the various uncertainties both in the experiments and in the computations, RBE calculations reproduce the self-broadening coefficients better than RB calculations for most lines of OCS for the two temperatures 200 and 298 K. Indeed, for RBE calculations, the mean difference $\varepsilon\% = \langle 100 \times |\text{exp} - \text{calc}| / \text{exp} \rangle$ is about 6.3% and 5.7% respectively for the temperatures 200 and 298 K. But, it is about 10.2% and 11.0 % respectively for 200 and 298 K for RB calculations of Bouanich et al. [6].

Table 3 presents the values of self-broadening coefficients for temperatures 200 K and 298 K obtained in this work as well as those reported in Ref. [6] corresponding to the ν_1 band of OCS.

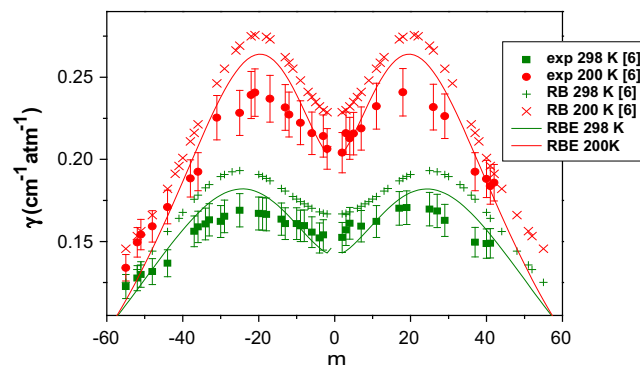


Fig. 4. Comparison between the experimental and theoretical results of Bouanich et al. [6] and the present theoretical results of self-broadening coefficients of the ν_1 band of OCS. The error bars (6%) are taken from Ref. [6].

Table 3
Theoretical and experimental values of self-broadening coefficients γ ($\text{cm}^{-1} \text{atm}^{-1}$) in the ν_1 band of OCS for temperatures 298 K and 200 K.

Lines	T = 298 K			T = 200 K			
	γ_{exp} [6]	γ_{RB} [6]	γ_{RBE}	γ_{exp} [6]	γ_{RB} [6]	γ_{RBE}	γ_{RBE}
R(54)	–	0.1251	0.1113	–	0.1456	–	0.1142
R(53)	–	–	0.1144	–	–	–	0.1184
R(52)	–	–	0.1175	–	–	–	0.1226
R(51)	–	0.1329	0.1206	–	0.1533	–	0.1270
R(50)	–	0.1357	0.1237	–	0.1563	–	0.1315
R(49)	–	–	0.1269	–	–	–	0.1360
R(48)	–	–	0.1300	–	–	–	0.1407
R(47)	–	0.1442	0.1331	–	0.1661	–	0.1455
R(46)	–	–	0.1362	–	–	–	0.1503
R(45)	–	–	0.1393	–	–	–	0.1550
R(44)	–	–	0.1424	–	–	–	0.1603
R(43)	–	0.1561	0.1454	–	0.1821	–	0.1655
R(42)	–	–	0.1484	–	–	–	0.1706
R(41)	–	–	0.1513	0.1858 (0.0111)	0.1912	–	0.1760
R(40)	0.1489 (0.0090)	0.1641	0.1542	0.1837 (0.0110)	0.1960	–	0.1812
R(39)	0.1487 (0.0090)	0.1677	0.1570	0.1881 (0.0113)	0.2009	–	0.1865
R(38)	–	–	0.1597	–	–	–	0.1919
R(37)	–	–	0.1623	–	0.2110	–	0.1972
R(36)	0.1496 (0.0090)	0.1757	0.1648	0.1925 (0.0115)	0.2161	–	0.2026
R(35)	–	0.1782	0.1672	–	0.2213	–	0.2079
R(34)	–	–	0.1694	–	–	–	0.2132
R(33)	–	0.1827	0.1715	–	–	–	0.2184
R(32)	–	0.1847	0.1735	–	–	–	0.2234
R(31)	–	–	0.1752	–	–	–	0.2284
R(30)	–	–	0.1768	–	0.2463	–	0.2332
R(29)	–	0.1896	0.1782	–	–	–	0.2377
R(28)	0.1629 (0.0100)	0.1908	0.1794	0.2263 (0.0136)	0.2552	–	0.2421
R(27)	–	–	0.1804	–	–	–	0.2461
R(26)	0.1686 (0.0101)	0.1925	0.1811	–	–	–	0.2499
R(25)	–	–	0.1816	0.2318 (0.0139)	0.2663	–	0.2533
R(24)	0.1697 (0.0102)	0.1932	0.1819	–	0.2692	–	0.2562
R(23)	–	–	0.1820	–	–	–	0.2588
R(22)	–	–	0.1818	–	–	–	0.2609
R(21)	–	–	0.1813	–	0.2749	–	0.2625
R(20)	–	–	0.1807	–	0.2757	–	0.2635
R(19)	–	0.1908	0.1798	–	–	–	0.2640
R(18)	0.1706 (0.0102)	0.1897	0.1786	–	–	–	0.2639
R(17)	–	0.1884	0.1773	0.2409 (0.0144)	0.2746	–	0.2633
R(16)	0.1702 (0.0102)	0.1870	0.1757	–	0.2731	–	0.2621
R(15)	–	–	0.1739	–	–	–	0.2603
R(14)	–	–	0.1720	–	–	–	0.2579
R(13)	–	0.1823	0.1699	–	–	–	0.2551
R(12)	–	0.1807	0.1676	–	0.2623	–	0.2517
R(11)	–	–	0.1653	–	0.2588	–	0.2479
R(10)	0.1622 (0.0097)	0.1774	0.1628	0.2324 (0.0139)	0.2552	–	0.2437
R(9)	–	0.1758	0.1603	–	–	–	0.2392
R(8)	–	0.1743	0.1578	–	0.2480	–	0.2345
R(7)	–	0.1729	0.1552	–	–	–	0.2296
R(6)	0.1593 (0.0096)	0.1715	0.1528	0.2188 (0.0131)	0.2411	–	0.2246
R(5)	–	0.1702	0.1504	–	0.2380	–	0.2197
R(4)	–	–	0.1481	0.2157 (0.0129)	0.2349	–	0.2150
R(3)	0.1611 (0.0097)	0.1680	0.1460	0.2128 (0.0127)	0.2322	–	0.2105
R(2)	0.1570 (0.0094)	0.1672	0.1443	0.2159 (0.0129)	0.2300	–	0.2067
R(1)	0.1525 (0.0091)	0.1668	0.1430	0.2041 (0.0122)	0.2287	–	0.2039
P(1)	–	–	0.1458	–	–	–	0.2079
P(2)	–	0.1668	0.1430	0.2064 (0.0124)	0.2287	–	0.2039
P(3)	0.1540 (0.0092)	0.1672	0.1443	0.2142 (0.0129)	0.2300	–	0.2067
P(4)	0.1522 (0.0091)	0.1680	0.1461	–	0.2322	–	0.2106
P(5)	–	–	0.1482	–	0.2349	–	0.2150
P(6)	0.1557 (0.0093)	0.1702	0.1504	0.2159 (0.0129)	0.2380	–	0.2197
P(7)	–	0.1715	0.1528	–	0.2411	–	0.2246
P(8)	0.1596 (0.0096)	0.1729	0.1553	–	–	–	0.2296
P(9)	0.1595 (0.0096)	0.1743	0.1578	0.2223 (0.0133)	0.2480	–	0.2340
P(10)	0.1609 (0.0096)	0.1758	0.1604	–	–	–	0.2392
P(11)	–	0.1774	0.1629	–	0.2552	–	0.2437
P(12)	–	–	0.1653	0.2273 (0.0136)	0.2588	–	0.2479
P(13)	0.1609 (0.0096)	0.1807	0.1677	0.2316 (0.0139)	0.2623	–	0.2517
P(14)	0.1636 (0.0098)	0.1823	0.1610	–	–	–	0.2551
P(15)	–	–	0.1721	–	–	–	0.2579
P(16)	–	–	0.1740	–	–	–	0.2603
P(17)	–	0.1870	0.1758	0.2369 (0.0142)	0.2731	–	0.2621
P(18)	0.1665 (0.0100)	0.1884	0.1773	–	0.2746	–	0.2633

Table 3 (continued)

Lines	T = 298 K			T = 200 K		
	γ_{exp} [6]	γ_{RB} [6]	γ_{RBE}	γ_{exp} [6]	γ_{RB} [6]	γ_{RBE}
P(19)	0.1669 (0.0100)	0.1897	0.1787	–	–	0.2639
P(20)	0.1671 (0.0100)	0.1908	0.1798	–	–	0.2640
P(21)	–	–	0.1807	0.2407 (0.0144)	0.2757	0.2635
P(22)	–	–	0.1814	0.2392 (0.0143)	0.2749	0.2625
P(23)	–	–	0.1818	–	–	0.2609
P(24)	–	–	0.1820	–	–	0.2588
P(25)	0.169 (0.0101)	0.1932	0.1820	0.2283 (0.0137)	0.2692	0.2562
P(26)	–	–	0.1817	–	0.2663	0.2533
P(27)	–	0.1925	0.1812	–	–	0.2499
P(28)	–	–	0.1804	–	–	0.2461
P(29)	0.1653 (0.0099)	0.1908	0.1794	–	0.2552	0.2421
P(30)	0.1622 (0.0097)	0.1896	0.1783	–	–	0.2377
P(31)	–	–	0.1769	0.2254 (0.0135)	0.2463	0.2332
P(32)	–	–	0.1753	–	–	0.2282
P(33)	0.1632 (0.0098)	0.1847	0.1735	–	–	0.2234
P(34)	0.1607 (0.0096)	0.1827	0.1716	–	–	0.2184
P(35)	–	–	0.1695	–	–	0.2132
P(36)	0.1589 (0.0095)	0.1782	0.1672	0.1925 (0.0115)	0.2213	0.2079
P(37)	0.1562 (0.0094)	0.1757	0.1649	–	0.2161	0.2026
P(38)	–	–	0.1624	0.1884 (0.0113)	0.2110	0.1972
P(39)	–	–	0.1598	–	–	0.1919
P(40)	–	0.1677	0.1571	–	0.2009	0.1865
P(41)	–	0.1641	0.1543	–	0.1960	0.1812
P(42)	–	–	0.1514	–	0.1912	0.1759
P(43)	–	–	0.1485	–	–	0.1707
P(44)	0.1368 (0.0082)	0.1561	0.1455	0.1710 (0.0103)	0.1821	0.1655
P(45)	–	–	0.1425	–	–	0.1604
P(46)	–	–	0.1394	–	–	0.1553
P(47)	–	–	0.1363	–	–	0.1504
P(48)	0.1317 (0.0079)	0.1442	0.1332	0.1592 (0.0095)	0.1661	0.1455
P(49)	–	–	0.1301	–	–	0.1407
P(50)	–	–	0.1269	–	–	0.1361
P(51)	0.1299 (0.0078)	0.1357	0.1238	0.1542 (0.0092)	0.1563	0.1315
P(52)	0.1277 (0.0077)	0.1329	0.1207	0.1495 (0.0090)	0.1533	0.1270
P(53)	0.1226 (0.0074)	–	0.1176	–	–	0.1227
P(54)	–	–	0.1145	–	–	0.1184
P(55)	0.1226 (0.0074)	0.1251	0.1114	0.1340 (0.0080)	0.1456	0.1142

4. Conclusion

We have performed predictions of self broadening coefficients of HCN and OCS as function of temperature. These calculations are based on the semiclassical model of Robert and Bonamy with exact trajectory (RBE) applied to the ν_1 and ν_2 bands of OCS and HCN respectively. For this work we had to determine the resonance functions. This task was achieved using the Starikov approximation, which takes into account the temperature dependence, to compute the self-broadening coefficients for the both collisional systems. These calculations reproduced nicely the evolution of pressure broadening coefficients with J rotational quantum number as well as the maximum of collision effectiveness for the considered temperature.

For the particular case of HCN-HCN system, we have regenerated theoretically the temperature exponent n consistently with experimental data. As a conclusion about this collisional system, the results of these calculations lead to a nice agreement with the experimental data.

For OCS-OCS collisional system with relatively weak electrostatic interactions, the RBE calculations permit to reduce significantly the disagreement between theoretical and experimental results.

For the both collisional systems, RBE approach appears more efficient to compute the self-broadening coefficients than RB formalism at various temperatures.

References

- [1] V.I. Starikov, *Opt. Spectrosc.* 112 (2012) 24.
- [2] D. Robert, J. Bonamy, *J. Phys. (Paris)* 40 (1979) 923.
- [3] C. Jellali, S. Galalou, F. Kwabia-Tchana, H. Aroui, *J. Mol. Phys.* 112 (2013) 1189.
- [4] S. Galalou, K. Ben Mabrouk, H. Aroui, F. Kwabia Tchana, F. Willaert, J.-M. Flaud, *J. Quant. Spectrosc. Radiat. Transfer* 112 (2011) 2750.
- [5] J.-P. Bouanich, G. Blanquet, *J. Quant. Spectrosc. Radiat. Transfer* 40 (1988) 205.
- [6] J.-P. Bouanich, G. Blanquet, J. Walrand, C.P. Courtney, *J. Quant. Spectrosc. Radiat. Transfer* 30 (1986) 295.
- [7] K.A. Ross, D.R. Willey, *J. Chem. Phys.* 122 (2005) 204308.
- [8] J.P. Bouanich, C. Boulet, A. Predoi-Cross, S.W. Sharpe, R.L. Sams, M.A.H. Smith, C.P. Rinsland, D. Chris Benner, V. Malathy Devi, *J. Mol. Spectrosc.* 231 (2005) 85.
- [9] V. Malathy Devi, D. Chris Benner, M.A.H. Smith, C.-P. Rinsland, A. Predoi-Cross, S.W. Sharpe, R.-L. Sams, C. Boulet, J.P. Bouanich, *J. Mol. Spectrosc.* 231 (2005) 66.
- [10] A.D. Bykov, L.N. Lavrentieva, L.N. Sinitza, *Atm. Ocean. Opt.* 5 (1992) 1127.
- [11] L.-D. Landau, E.M. Lifshitz, *Course of Theoretical Physics*, Pergamon, Oxford, 1958.
- [12] C. Yang, J. Buldyreva, I.-E. Gordon, F. Rohart, A. Cuisset, G. Mouret, R. Bocquet, F. Hindle, *J. Quant. Spectrosc. Radiat. Transfer* 109 (2008) 2857.
- [13] A. Predoi-Cross, V. Malathy Devi, P. Sutradhar, T. Sinyakova, J. Buldyreva, K. Sung, M.A.H. Smith, *J. Quant. Spectrosc. Radiat. Transfer* 177 (2016) 181.
- [14] M. Guinet, F. Rohart, J. Buldyreva, V. Gupta, S. Eliet, R.A. Motiyenko, L. Margules, A. Cuisset, F. Hindle, G. Mouret, *J. Quant. Spectrosc. Radiat. Transfer* 113 (2012) 1113.
- [15] C.J. Tsao, B. Burnutte, *J. Quant. Spectrosc. Radiat. Transfer* 2 (1961) 41.
- [16] C.P. Rinsland, V. Malathy Devi, M.A.H. Smith, D. Chris Benner, S.W. Sharpe, R.L. Sams, *J. Quant. Spectrosc. Radiat. Transfer* 82 (2003) 343.
- [17] M.A.H. Smith, C.P. Rinsland, T.A. Blake, R.L. Sams, D. Chris Benner, V. Malathy Devi, *J. Quant. Spectrosc. Radiat. Transfer* 109 (2008) 922.
- [18] V. Malathy Devi, D. Chris Benner, M.A.H. Smith, C.P. Rinsland, A. Predoi-Cross, S.W. Sharpe, R.L. Sams, *J. Mol. Spectrosc.* 82 (2003) 319.
- [19] S. Matton, F. Rohart, R. Bocquet, G. Mouret, D. Bigourd, A. Cuisset, *J. Mol. Spectrosc.* 239 (2006) 182.
- [20] M.A. Koshelev, M.Y. Tretyakov, F. Rohart, J.-P. Bouanich, *J. Chem. Phys.* 136 (2012) 124316.
- [21] J. Buldyreva, J. Bonamy, D. Robert, *J. Quant. Spectrosc. Radiat. Transfer* 62 (1999) 321.
- [22] Q. Ma, R.H. Tipping, R.R. Gamache, *J. Mol. Phys* 108 (2014) 2225.

- [23] J. Buldyreva, N. Lavrentieva, V. Starikov, *Collisional Lines Broadening and Shifting of Atmospheric Gases*, World Scientific, Imperial College Press, London, 2010.
- [24] U. Fano, G. Racah, *Irreducible Tensorial Sets*, Academic Press Inc., New York, 1959.
- [25] A. Belafhal, A. Fayt, G. Guelachvili, *J. Mol. Spectrosc.* 174 (1995) 1.
- [26] L.S. Masudiki, J.G. Lahaye, A. Fayt, *J. Mol. Spectrosc.* 148 (1991) 281.
- [27] F.H. De Leeuw, A. Dymanus, *Chem. Phys. Lett.* 7 (1970) 288.
- [28] U.G. Jorgensen, J. Almlof, B. Gustafsson, M. Larsson, P. Siegbahn, *J. Chem. Phys.* 83 (1985) 3034.
- [29] C.G. Gray, K.E. Gubbins, in: *Theory of Molecular Fluids, Fundamentals*, vol. I, Oxford University Press, New York, 1984.
- [30] J.O. Hirschfelder, C.F. Curtiss, R.B. Bird, *Molecular Theory of Gases and Liquids*, John Wiley & Sons, New York, 1967.
- [31] A.G. Maki, G.C. Mellau, S. Klee, M. Winnewisser, W. Quapp, *J. Mol. Spectrosc.* 202 (2000) 67.
- [32] J. Hietanen, K. Jolma, V.M. Horneman, *J. Mol. Spectrosc.* 127 (1988) 272.
- [33] S.V. Churakov, M. Gottschalk, *Geochim. Cosmochim. Acta* 67 (2001) 2397.
- [34] J. Pourcin, A. Jacquemoz, A. Fournel, H. Sielmann, *J. Mol. Spectrosc.* 231 (2005) 66.